Long-wavelength phonon dynamics in incommensurate $Bi_2Sr_2CaCu_2O_{8+\delta}$ crystals by Brillouin light scattering spectroscopy

B. D. E. McNiven, J. P. F. LeBlanc, and G. T. Andrews*

Department of Physics and Physical Oceanography, Memorial University of Newfoundland and Labrador, St. John's, Newfoundland & Labrador, Canada A1B 3X7

(Received 4 February 2022; revised 12 July 2022; accepted 22 August 2022; published 31 August 2022; corrected 1 September 2022)

Room-temperature phonon dynamics in crystals of the high-T_c superconductor $Bi_2Sr_2CaCu_2O_{8+\delta}$ were probed using Brillouin light scattering spectroscopy. Six distinct bulk acoustic modes were observed and identified: two quasilongitudinal bulk modes and four quasitransverse bulk modes. A peak at a frequency shift of ∼95 GHz with behavior reminiscent of an optic phonon was also observed in the spectra. The existence and nature of these modes is a manifestation of the incommensurate structure of $Bi_2Sr_2CaCu_2O_{8+\delta}$ and suggests that it may be categorized as a so-called composite incommensurate crystal comprised of two weakly interacting sublattices. A mass ratio of $m_1/m_2 = 2.8$ obtained from the two measured quasilongitudinal acoustic velocities led to sublattice assignments of $Bi_2Sr_2O_4$ and $CaCu_2O_4$. Two surface acoustic modes were also observed in the spectra, the number and character of which suggest that the incommensurate structure in the near-surface region is disrupted due to microscopic-scale damage and/or the presence of defects. The Brillouin data also place an upper limit of ∼10 GHz on the crossover frequency between commensurate and incommensurate phonon dynamics.

DOI: 10.1103/PhysRevB.106.054113

I. INTRODUCTION

Quasiparticle dynamics in incommensurate systems are not well understood, with the scarcity of knowledge being particularly acute for long-wavelength acoustic phonons. While the "usual" phonon dispersion for a typical commensurate crystal consists of 3*N*-3 optic and three acoustic phonon modes, where *N* is the number of atoms in the unit cell, theoretical studies predict modifications to the phonon dispersions of incommensurate crystals due to their unique structure [1–6]. Moreover, complementary experimental work on acoustic phonon dynamics in such systems is limited despite the fact that many have incommensurate phases at ambient temperatures, making them prime candidates for laboratory investigation. The crystalline form of high-temperature superconductor $Bi_2Sr_2CaCu_2O_{8+\delta}$ (Bi-2212) is one such material [7–9].

Experiments aimed at probing acoustic phonon dynamics in Bi-2212 reveal complex dispersion with branch crossings and the unexpected absence or presence of particular modes arising from the incommensurate structure. For example, inelastic neutron scattering results suggest that coupling of longitudinal acoustic phonons to electrons is limited to zone center phonons by branch anticrossings, and that low-energy spectral weight near a charge density wave ordering wave vector arises from an extra low-lying acoustic phonon branch emanating from a nearby superlattice modulation reflection [10]. Possibly consistent with this second suggestion is the observation of two (instead of the usual one) longitudinal acousticlike modes along the incommensurate direction in another neutron scattering study [11]. Interestingly, only one longitudinal mode was measured in this direction in ultrasonic pulse-echo experiments conducted at 7.5 MHz [12]. These last two observations suggest an undiscovered crossover from two propagating longitudinal modes to one such mode in the 10 MHz–150 GHz frequency regime inaccessible to these two techniques. Furthermore, neutron scattering experiments conducted along the incommensurate direction in Bi-2212 detected only one transverse mode instead of the two that were expected [11]. Additionally, Ref. [10] indicates that multiple phonon branches beyond a normal limit can be expected for Bi-2212. Given that the GHz-frequency regime remains largely unexplored, it is likely that one or more of these branches could exist in this frequency range.

This paper reports on Brillouin light scattering experiments on high-quality single crystals of Bi-2212, the need for which has been repeatedly articulated in the literature [11,13]. By probing with sub-GHz resolution a frequency range inaccessible to ultrasonics and neutron scattering techniques, the results of this study provide insight into the dynamics of long-wavelength hypersonic phonons in Bi-2212. In particular, the incommensurate structure of Bi-2212 is manifested in the Brillouin spectrum through the presence of multiple acoustic phonon peaks in excess of those expected for a typical crystal. This observation places an upper limit of ∼10 GHz on the "separate sublattice-to-standard single crystal" crossover frequency and suggests that Bi-2212 is more accurately described as a composite incommensurate crystal rather than a modulated incommensurate crystal. Moreover, quasilongitudinal phonon velocities determined in this work permit identification of the two sublattices that comprise the incommensurate Bi-2212 crystal. The damping-out, with increasing proximity to the incommensurate direction, of a previously

*tandrews@mun.ca

unreported low-lying opticlike mode at ∼95 GHz may be another manifestation of the incommensurate character of Bi-2212. Based on the above observations, this Brillouin scattering study reveals the incommensurate nature of Bi-2212.

II. EXPERIMENTAL DETAILS

Brillouin spectroscopy is an inelastic laser light scattering technique used to probe thermally excited acoustic phonons in condensed-matter systems. In this technique, monochromatic light is directed at the sample of interest, and the light scattered in some predefined direction is frequency-analyzed. Depending upon the nature of the sample and the scattering geometry, the resulting spectrum may contain peaks due to surface, interface, film-guided, and/or bulk acoustic phonons in the target material at frequencies shifted from that of the incident light due to the inelastic nature of the scattering. Measurement of these peak shifts, which are typically in the GHz range, yield phonon velocities from which elastic moduli may be determined. Knowledge of Brillouin peak widths gives information on phonon attenuation and, in opaque materials like Bi-2212, optical constants [14]. Further details on the instrumentation and scattering geometries employed, the types of excitations probed, the methods used to facilitate mode identification, and the variety of systems that may be studied using this technique are provided in several comprehensive review articles [15–17].

Brillouin scattering experiments were performed at room temperature using a 180° backscattering geometry on (001)-oriented flakes of Bi-2212 exfoliated from three parent crystals with critical temperatures of 78, 90, and 91 K. Incident light was provided by a single-mode frequency-doubled Nd:YVO_4 laser emitting at a wavelength of $\lambda_i = 532$ nm. The beam was horizontally ("p") polarized by use of a half-wave plate and then passed through neutral density filters to reduce the power at the sample to ∼10 mW to minimize heating due to optical absorption. The scattered light was collected and collimated by a high-quality camera lens with an aperture setting of $f/2.8$ and subsequently focused onto the entrance pinhole of a six-pass tandem Fabry-Pérot interferometer using an $f = 40$ cm lens. The pinhole diameter was set to 300 or 450 μm, with the former being used when the central elastic peak width needed to be reduced to reveal Brillouin peaks at very small frequency shifts. A photograph and a schematic diagram of the complete setup used in these experiments are given in Ref. [18].

Brillouin spectra were collected for angles of incidence ranging from 10° to 75°, corresponding via Snell's law to internal angles of refraction, and therefore probed phonon propagation directions, from ∼5° to ∼29° from the crystallographic c-axis. It was not possible to obtain spectra for angles of incidence <10° due to the signal being swamped by intense reflected light.

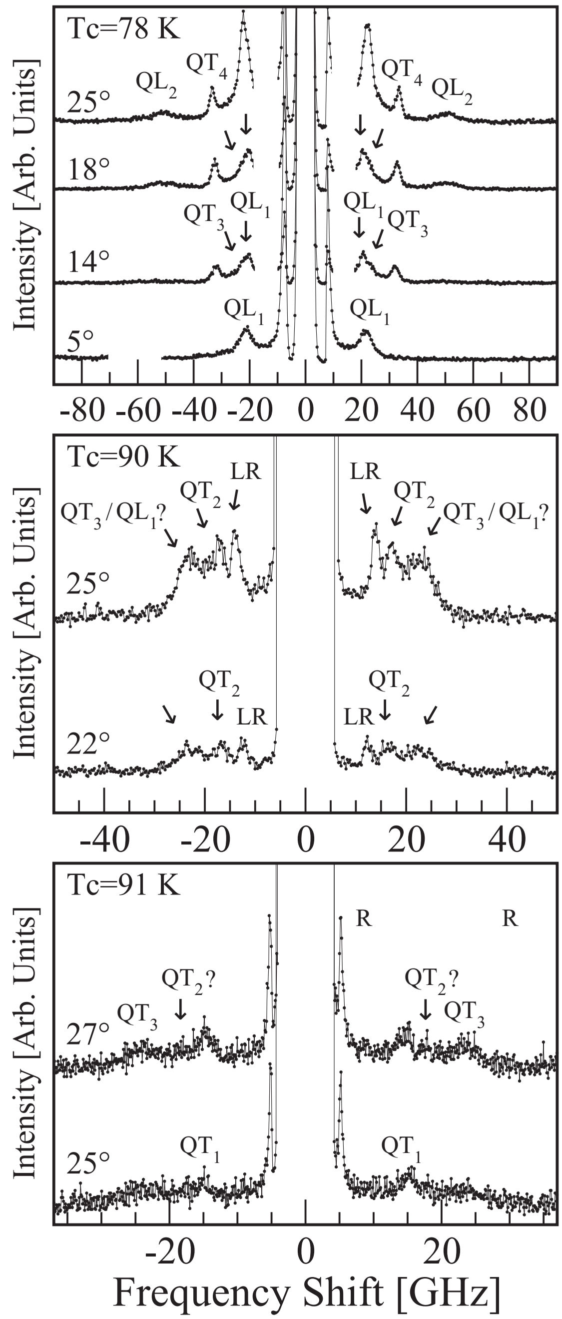

FIG. 1. Room-temperature Brillouin spectra of Bi-2212 crystals with $T_c = 78$ K (upper panel), 90 K (middle panel), and 91 K (lower panel) for phonon propagation directions as measured from the crystallographic c-axis. Eight acoustic modes are observed. R, surface Rayleigh; LR, longitudinal surface resonance; QT_i, quasitransverse; QL_i, quasilongitudinal. The QT_3/QL_1? peak in the middle panel is labeled in this way because it is not clear if it is QT_3 or QL_1 due to the similarity in shifts. The assignment of the QT_2? peak in the lower panel to the QT_2 mode is not definitive because, although it appears at the same shift as the QT_2 peak in the middle panel, it is barely discernible in the spectrum. Note: In the upper panel, QT_1 is omitted due it being overshadowed by a strong signal from sample mounting tape. The region near 60 GHz is omitted in the 5° spectrum due to a known experimental artefact. For all spectra shown in this figure, the incident light was p-polarized, and no polarizer was present in the scattered beam.

III. RESULTS AND DISCUSSION

A. Brillouin spectra—General features

Figure 1 shows representative Brillouin spectra of three Bi-2212 crystals. Eight different Brillouin peak doublets (labeled R, LR, QT_i with $i = 1$–4, and QL_j with $j = 1$–2) are

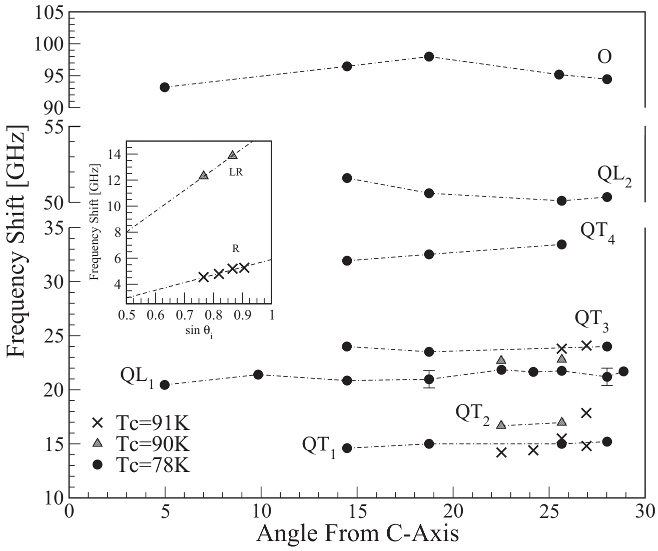

FIG. 2. Brillouin shift vs propagation direction for peaks due to bulk quasitransverse (QT_1, QT_2, QT_3, and QT_4), quasilongitudinal (QL_1, QL_2) acoustic phonon modes, and a low-lying optic mode (O). The inset shows the Rayleigh (R) and longitudinal surface resonance (LR) acoustic phonon modes fitted through the origin. Omitted error bars are approximately the size of the associated data point symbols.

present in the spectra, with the number and intensity of these modes varying with angle of incidence and from sample to sample. The overall quality of the spectra is strongly sample-dependent, with the $T_c = 78$ K sample giving those of the highest quality. In fact, spectra like those shown in the top panel of Fig. 1 were obtained on multiple flakes of this sample. Spectra obtained from the other two crystals are only of fair quality despite single-spectrum collection times of $\geqslant 20$ h. These differences may be due to crystal quality effects possibly related to the growth method. In any case, the Brillouin spectra in this work are of the highest quality yet obtained for Bi-2212.

The directional dependence of the Brillouin peak frequency shifts is shown in Fig. 2. For the lowest angles of incidence (i.e., directions closest to the c-axis) only peak QL_1 is present in the spectra. At larger angles of incidence ($>14^\circ$ from the c-direction), the R, LR, QT_1, QT_2, QT_3, QT_4, and QL_2 peaks appear in the spectra of one or more of the three samples. It is noted that the large width and asymmetry of the peak at ~21 GHz for the $T_c = 90$ K sample (the unlabeled peak indicated by arrows in the middle panel of Fig. 1) suggests that it may in fact be two closely spaced peaks due to the QT_2 and QL_1 modes, similar to what was observed for the $T_c = 78$ K sample (see the top panel of Fig. 1). With the exception of the R and LR peaks (see Fig. 2, inset), the peak shifts show only a small variation with propagation direction. This apparent lack of appreciable anisotropy is primarily an artefact of the relatively limited angular ranges probed, over which a large variation in shift is not expected. Variation in the peak frequency shift of similar magnitude over comparable ranges of angles from the crystallographic c-axis was observed for bulk acoustic modes in Brillouin scattering studies of several other layered materials including V_2O_5 [19], $CdPS_3$ [20], and muscovite mica [21]. Acoustic modes in some artificial hybrid layered systems, however, can show substantial anisotropy over a relatively small range of directions [22].

B. Mode assignment

1. Surface acoustic phonon modes

The shifts of the peaks labeled R and LR show a strong linear dependence on the sine of the angle of incidence, and they are therefore assigned to the Rayleigh surface mode and longitudinal resonance, the latter being observed only in the spectra of the sample with $T_c = 90$ K. Accordingly, the velocities of these modes were determined by fitting the Brillouin equation for surface modes, $f_S = 2V_S \sin\theta_i/\lambda_i$, where V_S is the velocity of the Rayleigh mode ($S = R$) or the longitudinal resonance ($S = LR$), to the experimental frequency shift (f_S) versus $\sin\theta_i$ data. The velocities, determined from the slopes of the lines of best fit, were found to be $V_R = 1570 \pm 20$ m/s and $V_{LR} = 4260 \pm 40$ m/s for the $T_c = 91$ and 90 K samples, respectively, and they are comparable to those found in a previous Brillouin scattering study of Bi-2212 [23]. The widths of the R and LR peaks are also noticeably smaller than those of the other peaks, further supporting the assignment of these peaks to surface modes.

2. Bulk quasitransverse acoustic phonon modes

Peaks QT_1, QT_2, QT_3, and QT_4 are assigned to quasitransverse acoustic modes because the shifts show little dependence on direction and because they are absent in small-incident-angle spectra [24] and show an overall increase in intensity with increasing angle of incidence. Moreover, the frequency shifts of QT_1 and QT_3 are close to those of peaks identified as quasitransverse acoustic modes in previous Brillouin scattering experiments [23], although it is also possible that the peak identified as the fast quasitransverse mode in Ref. [23] is actually QL_1 due to its proximity to QT_3, as shown in the top panel of Fig. 1. Further support for this mode assignment is provided by ultrasonics measurements on ceramic Bi-2212 samples with the c-axis of grains preferentially aligned, which give transverse mode velocities within $\leqslant 10\%$ of those of QT_1 and QT_2 (see Table I). Incidentally, the longitudinal acoustic mode velocity measured along the c-axis in the same study is also in excellent agreement with that of QL_1 determined in the present work [25].

It is also worth noting here that the close proximity of QT_2 and QT_3 to QL_1 (a range spanning ~6 GHz) could explain why inelastic neutron scattering experiments have consistently measured only one transverse acoustic mode [11], since that technique lacks the resolution necessary to resolve two peaks separated by only a few GHz.

3. Bulk quasilongitudinal acoustic phonon modes

The most surprising result of the present study is the presence of two distinct quasilongitudinal bulk mode peaks (QL_1 and QL_2) in the Brillouin spectrum of Bi-2212, neither of which was seen in previous Brillouin scattering studies [23,26,27]. The longitudinal character of these modes was confirmed by polarization analysis of the scattered light. To perform this analysis, it was first noted that for normally incident p-polarized light, the light scattered from longitudinal

TABLE I. Room-temperature transverse (V_{T_i}) and longitudinal (V_{L_i}) bulk acoustic phonon velocities along various directions for crystalline Bi-2212. V_L is the longitudinal acoustic phonon velocity in the $q \to 0$ limit determined by (i) ultrasonics or Brillouin scattering measurement, or (ii) Eq. (1) through knowledge of velocities V_{L_1} and V_{L_2}, and sublattice masses m_1 and m_2, with use of the latter method indicated by a footnote. Note: V_{T_i} and V_{L_i} for the present Brillouin scattering studies refer to quasitransverse and quasilongitudinal velocities, respectively. Bulk phonon velocities determined in the present work have an associated ∼5% uncertainty.

Technique	Study	T_c (K)	Direction	V_{T_1} (m/s)	V_{T_2} (m/s)	V_{T_3} (m/s)	V_{T_4} (m/s)	V_{L_1} (m/s)	V_{L_2} (m/s)	V_L (m/s)
Brillouin Light Scattering	Present work	78	5° from [001]							2700
			28° from [001]	1900		3200	4400	2700	6700	
		90	26° from [001]		2300					
		91	27° from [001]	2000	2400					
	Ref. [23][a]	78–92	[001]							3413
			[010]							4380
Inelastic Neutron Scattering	Ref. [11]		[001]	1830						
			[010]					2400	5900	4700[e]
	Ref. [10][b]		[001]	1780						2440
Ultrasonic	Refs. [12,34][c]	84.5	[010]		2460					4150
	Ref. [25][d]		[001]	1750						2670
			In (001) plane	1740	2460					4370

[a]Estimated from longitudinal resonance measurements, uncertainties are ∼5%.
[b]Estimated from inelastic neutron scattering measurements at $T \leqslant T_c$.
[c]Estimated from velocity vs temperature curves.
[d]Velocities obtained from polycrystalline samples that show a preferred grain orientation.
[e]Estimated from data in Ref. [11] substituted into Eq. (1).

and transverse bulk modes is *p*- and *s*-polarized, respectively [28]. Modes with longitudinal polarization will therefore be present in spectra for which the incident and scattered light are *p*-polarized (*pp* configuration) and absent when the incident light is *p*-polarized and the scattered light is *s*-polarized (*ps* configuration). Although it was not possible to obtain spectra for normally incident light, QL_1 was observed in *pp*-spectra obtained at an internal angle of incidence of 6° to the crystallographic *c*-axis, but not in the corresponding *ps*-spectra, verifying that it is a longitudinal mode (see Fig. 3). A similar result was obtained for QL_2, but for an angle of 19° from the *c*-axis because this mode could not be readily observed at lower angles (see Figs. 1 and 2). It is noted that QL_1 is still visible but at reduced intensity in the 19° *ps*-polarized spectrum due to the fact that this mode has some transverse character for such general directions of propagation.

The fact that the QL_1 peak is quite intense in low incident angle spectra also supports its assignment to a quasilongitudinal acoustic mode because strong peaks due to quasitransverse modes are not expected to be present in Brillouin spectra under these circumstances [24]. Furthermore, the rather large shift of the QL_2 peak (∼50 GHz) is consistent with this assignment.

4. Low-lying optic phonon mode

Figure 4 shows that the Brillouin spectra contain a weak peak at $\sim \pm 95$ GHz. The large frequency shift of this peak relative to others in the spectrum and the intensity difference between the Stokes and anti-Stokes scattering suggest that it is due to an extremely low-lying optic phonon mode. As the right panel of Fig. 4 shows, this peak is strongest for phonon propagation directions close to the commensurate *c*-axis

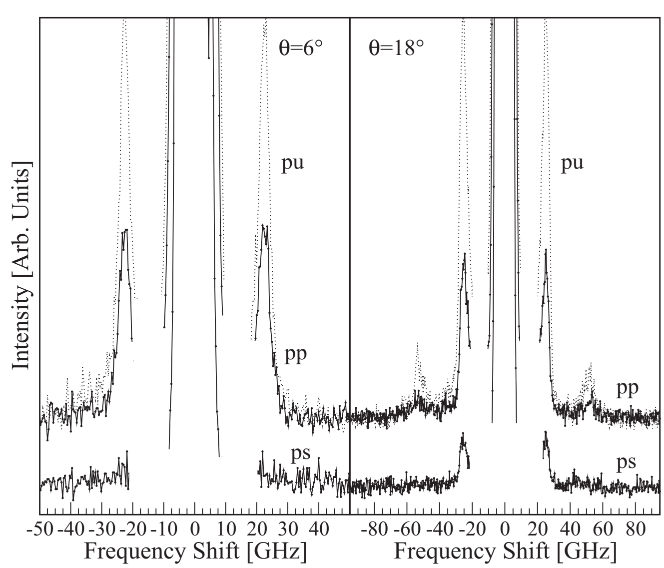

FIG. 3. Polarized spectra of a Bi-2212 crystal with $T_c = 78$ K. The notation "XY," where $X, Y = u$, p, or s, indicates the polarization state of the incident and scattered light, respectively. u, p, and s refer to unpolarized, p-polarized, and s-polarized light, respectively. Note: The spectral region inside 20 GHz was removed because it contained a strong signal from sample mounting tape.

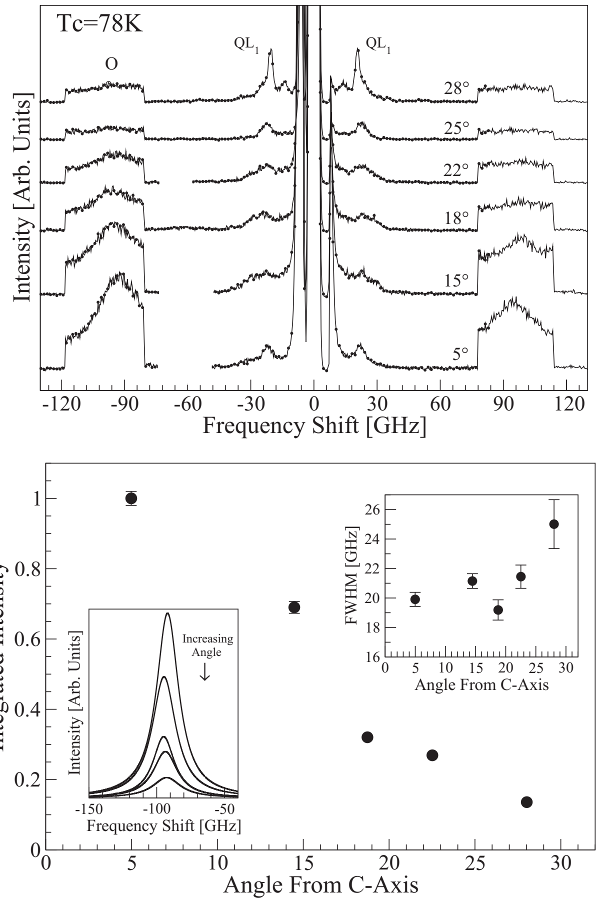

FIG. 4. Top panel: room-temperature Brillouin spectra of single-crystal Bi-2212. The region from $\sim\pm 80$ GHz to $\sim\pm 120$ GHz was segmented such that the collection time per channel in this region was $10\times$ that in the remainder of the spectrum. Note: to avoid confusion, portions of some spectra are omitted due to a known artefact at $\sim$60 GHz. Bottom panel: integrated intensity of an apparent low-lying opticlike mode vs propagation direction as measured from the crystallographic c-axis. Left inset: peak intensity vs frequency shift for the same mode. Right inset: FWHM of low-lying opticlike mode.

(5° from the c-axis for $\theta_i = 10°$) and becomes progressively less intense as the propagation direction moves away from this direction toward the ab-plane, being weakest at $\sim$28° ($\theta_i = 70°$) from the c-axis, the largest angle probed. This decrease in integrated intensity is accompanied by a corresponding decrease in peak intensity and an increase in peak width (FWHM), as seen in the left- and right-hand insets of Fig. 4, respectively. The peak frequency shift remains relatively constant over the range of directions probed, varying by a maximum of only 2–3 % from its mean value of 95.5 GHz (see Fig. 2). It was also noted that this peak appeared in both pp- and ps-spectra collected at angles of incidence very close to the c-axis (<5°), suggesting that it is not due to a typical acoustic mode.

C. Incommensurate structure

The unusual Brillouin scattering results described above are a consequence of the incommensurate nature of Bi-2212. Surprisingly, this is the first time that the incommensurate character of Bi-2212 has been observed in the Brillouin spectrum—previous studies make no mention of its incommensurate structure, nor are there any obvious signatures of it in published spectra. This is primarily because the spectral region beyond shifts of ±30 GHz was not explored, but may also be related to recent improvements in crystal quality. As seen in Fig. 1, the presence of peaks in excess of those expected for a typical commensurate crystal is highly sample dependent and therefore may be a sensitive function of doping. In fact, the presence or absence of some optic phonon peaks in Raman spectra of Bi-2212 and other cuprate systems has been shown to depend on doping [29,30].

1. Signatures

The most striking manifestation of the incommensurate structure of Bi-2212 in the Brillouin spectrum is the presence of two peaks, QL_1 and QL_2, due to quasilongitudinal modes. These peaks are both present in spectra for phonon propagation directions between $\sim$15° and $\sim$28° from the c-axis. In contrast, only QL_1 is present for propagation directions within $\sim$10° of the commensurate c-direction (see Fig. 2). This can be explained by noting that for phonon propagation directions at relatively large angles to the c-axis, the projection of the probed phonon wave vector in the ab plane, and therefore the component of $\vec{q}$ along the incommensurate b-direction, will be appreciable, resulting in the presence of spectral features due to the incommensurate nature of Bi-2212, including QL_2. As the direction of probed phonon propagation approaches the c-axis, the b-component of $\vec{q}$ approaches zero and the incommensurate nature is no longer apparent in the spectrum, accounting for the absence of QL_2 in small-angle spectra. The situation just described will be true unless, by coincidence, $\vec{q}$ happens to lie precisely in the ac plane, in which case the b-component will be zero. This is, however, extremely unlikely.

The presence of two quasilongitudinal modes due to incommensurate structure in Brillouin spectra of Bi-2212 is consistent with the results of neutron scattering studies in which two longitudinal acoustic modes were observed along the incommensurate b-direction in Bi-2212 and Bi-2201 [11,13]. As Table I shows, the velocities of these modes for Bi-2212 were found to be 2400 and 5900 m/s, and they are comparable in magnitude to, and in the same ratio as, the velocities of the QL_1 and QL_2 modes (2700 ± 100 and 6700 ± 300 m/s at 28° from the c-axis, the closest direction to the b-axis probed; calculated using $V_B = f_B\lambda_i/2n$, where B refers to bulk and $n = 2.0 \pm 0.1$ at 532 nm, where the estimated uncertainty was taken as the spread in published refractive index values of $1.9 \leqslant n \leqslant 2.1$ [31–33]). The fact that the velocities determined in the neutron scattering experiments are lower than those of QL_1 and QL_2 may seem counterintuitive given that the magnitudes of the latter are partially determined by the elastic constant(s) associated with the weak interlayer bonding in Bi-2212. This can be reconciled by noting both the lower resolution of neutron scattering in the $q \to 0$ limit when compared to Brillouin scattering, and the fact that it probes acoustic phonons at much higher q values where the velocity is typically expected to be lower due to a reduction in dispersion curve slope with increasing q. This potential for the pertinent analytical techniques to measure different velocity values for a given mode due to changes in dispersion curve slope was also highlighted in Ref. [6]. Underestimation of refractive index n could also contribute to the Brillouin scattering velocities being larger than those obtained by neutron scattering. A refractive index that is 5% higher than that used here (i.e., 2.1 instead of 2.0, as dictated by the uncertainty of 0.1) would give Brillouin velocities V_B that are ∼5% lower and therefore closer to those measured by inelastic neutron scattering [11].

A second signature of the incommensurate structure of Bi-2212 is the existence of four distinct QT modes for some propagation directions (see Fig. 2). The observation of twice as many QT peaks (i.e., two sets of 2 QT peaks) as would be expected for a commensurate crystal makes sense because of the two different periodicities associated with the incommensurate structure of Bi-2212. This reasoning also explains nicely the presence of two QL peaks in the Bi-2212 spectrum instead of the lone QL peak normally observed in the spectrum of a commensurate crystal.

The behavior of the low-lying optic mode may also be a consequence of the incommensurate structure of Bi-2212. The trends in integrated intensity, peak intensity, FWHM, and peak frequency shift described above (see Sec. III B 4) collectively suggest that the incommensurate structure of Bi-2212 causes this mode to be damped out. This reasoning may also explain why this mode is not observed in studies for which the primary or sole focus is phonon dynamics in the vicinity of the incommensurate b-direction.

The observation of a single Rayleigh surface mode peak (R) and a single longitudinal surface resonance peak (LR) in the Brillouin spectra suggests that the Bi-2212 surface does not possess incommensurate structure. Consistent with this conclusion is that both of these modes have velocities that are quite similar to those obtained in previous Brillouin studies of Bi-2212 for which no incommensurability was observed [23], and in the case of the LR mode, a velocity ($V_{LR} = 4260$ m/s) that is nearly identical to the $q \to 0$ limit velocity obtained by ultrasonics along the incommensurate direction ($V_L = 4150$ m/s [12,34]), and quite different from V_{QL_1} or V_{QL_2} (see Table I). The reason for the absence of incommensurate surface structure is not known, but it may be that the pristine incommensurate structure that exists in the bulk of the crystal is disturbed in the near-surface region due to microscopic-scale roughness and/or damage, effects to which Brillouin scattering is highly sensitive [35]. In fact, an early Brillouin study on crystalline Bi-2212 for which no signatures of incommensurability were observed notes the presence of surface roughness and points to it as a major contributor to poor spectrum quality [26]. It is also conceivable that adsorbed contaminants could be responsible for disrupting the incommensurate structure at the surface, although this seems unlikely given that one R peak rather than a set of two was observed in He-atom scattering spectra of Bi-2212 crystal surfaces prepared by cleaving under UHV conditions [36].

2. Consistency with the composite incommensurate crystal model

The existence of two sets of three acoustic phonon modes [$2\times(1\ QL+2\ QT)$] suggests that Bi-2212 may be categorized as a composite incommensurate crystal, a class of aperiodic crystal in which the incommensurability arises from interpenetrating, mutually incommensurate sublattices [37] and for which, in contrast to modulated incommensurate crystals, an average periodicity cannot be defined [2]. This result also suggests that the two sublattices that comprise Bi-2212 are weakly interacting. In fact, two independent sets of phonon branches are observed in a model consisting of two interpenetrating atomic chains of different periods when there is no coupling between the chains [2]. Moreover, while there do not appear to be any explicit theoretical or experimental results on acoustic phonon dispersion in composite incommensurate crystals for general phonon propagation directions, the results obtained in the present work do bear some similarities to the results of previous studies of acoustic phonon dynamics in high-symmetry directions in Bi-2212. In particular, the presence of two distinct longitudinal acoustic modes is consistent with the predictions of the incommensurate composite model and also with inelastic neutron scattering results [11,13].

Knowledge of the sublattice velocities V_{QL_1} and V_{QL_2} makes it possible to identify the composition of the two sublattices via their estimated mass ratio [38],

$$\frac{m_1}{m_2} = \frac{V_{QL_2}^2 - V_{q\to 0}^2}{V_{q\to 0}^2 - V_{QL_1}^2}, \tag{1}$$

where $V_{q\to 0}$ velocity is the longitudinal mode velocity in the $q \to 0$ limit, and m_i and V_{QL_i}, $i = 1, 2$, are the mass and quasilongitudinal velocity of the ith sublattice, respectively. Given that ultrasonic experiments measure only a single longitudinal velocity equal to 4150 m/s in the MHz range in the incommensurate b-direction [12,34], this velocity can be taken as $V_{q\to 0}$. Using this, along with $V_{QL_1} = 2700 \pm 100$ m/s and $V_{QL_2} = 6700 \pm 300$ m/s in Eq. (1), gives $m_1/m_2 = 2.8 \pm 0.5$. While the relatively large uncertainty in m_1/m_2 permits a number of possible sublattice pair candidates, that of $Bi_2Sr_2O_4$ with mass 658 u and $CaCu_2O_4$ with mass = 232 u (neglecting δ) gives $m_1/m_2 = 2.8$, in excellent agreement with the value obtained from Eq. (1). This result is nearly a factor of 2 larger than the value of $m_1/m_2 = 1.5$ obtained in neutron scattering studies, which led to sublattice assignments of $Bi_2SrO_{2+\delta}$ and $SrCaCu_2O_6$ [11].

3. Crossover frequency

Figure 5 schematically shows the relatively low-q portion of the acoustic phonon dispersion (low-lying optic mode not shown) for Bi-2212 for a general propagation direction as informed by collective consideration of ultrasonics [12,34], inelastic neutron scattering [11], and current Brillouin scattering data. At very small q, as probed by ultrasonic techniques at frequencies of ∼10 MHz, two transverse modes and a single longitudinal mode (QT_1, QT_2, and QL_1) would be observed as for a typical commensurate crystal. That this is the case can be inferred from the "Ultrasonics" data at the bottom of Table I. At a critical wave vector, q_c, higher than has been probed in ultrasonics experiments, there is a crossover from three to six propagating bulk acoustic modes due to the incommensurate structure of Bi-2212. These six modes are those observed in the present Brillouin scattering study, which probed phonons with a q-value greater than q_c and

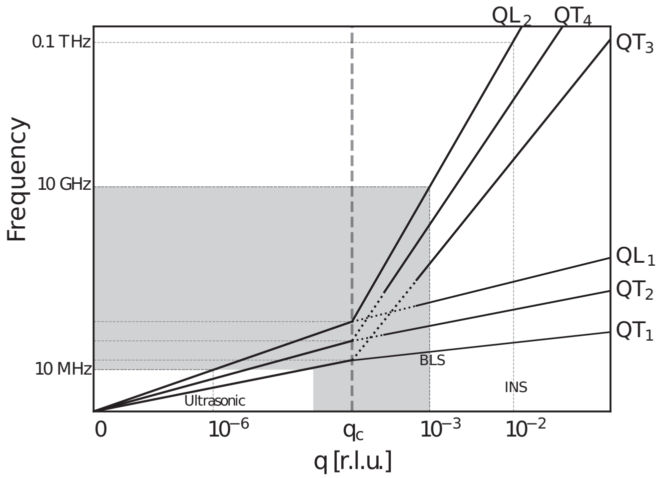

FIG. 5. Simplified schematic representation of low-q acoustic phonon dispersion for Bi-2212 for a general direction of propagation. q_c is the wave vector corresponding to the crossover frequency between commensurate and incommensurate dynamics. Approximate values of phonon wave vectors (q) in r.l.u. are shown for ultrasonic, Brillouin, and neutron scattering experiments.

with frequencies on the order of ~10 GHz. The frequency(ies) at which the crossover occurs therefore lie(s) in the range 10 MHz–10 GHz, one to four orders of magnitude higher than the value of ~1 MHz predicted by theory for the crossover from one to two propagating longitudinal acoustic modes in the Hg-chain compounds $Hg_{3+\delta}AsF_6$, the only composite incommensurate crystal system for which an estimate of crossover frequency has been provided [38]. Intuitively, one might expect an analogous crossover at comparable frequencies for quasitransverse modes, but this does not seem to be discussed in the literature. Inelastic neutron scattering accesses phonons with still higher q values in the $q > q_c$ region but with lower frequency resolution than Brillouin spectroscopy. While there do not appear to be any measurements for directions other than along crystallographic axes, two longitudinal phonons were observed in the incommensurate b-direction in neutron scattering experiments on Bi-2212 [11], consistent with the scheme shown in Fig. 5. One of the consequences of the lower resolution, however, is that modes that are closely spaced in frequency may not be resolved in neutron scattering experiments. This could explain the absence of otherwise anticipated modes in previous neutron scattering studies of Bi-2212 [11].

IV. CONCLUSION

In summary, low-frequency phonon dynamics of Bi-2212 single crystals were studied using Brillouin light scattering spectroscopy. From collected spectra, two quasilongitudinal acoustic and four quasitransverse acoustic phonon modes were observed, with the former in agreement with previous inelastic neutron scattering studies [11] indicating that Bi-2212 is a composite incommensurate crystal. The measured frequency shifts of the six bulk acoustic phonon modes allowed for the assignment of each mode to a given sublattice, while the quasilongitudinal acoustic phonon velocities were used to propose sublattice assignments of $Bi_2Sr_2O_4$ and $CaCu_2O_4$. Furthermore, a low-lying opticlike mode was also observed and appears to be another manifestation of the incommensurate nature of Bi-2212. The rich and highly unusual Brillouin spectra obtained here make it clear that further attention is warranted to fully understand phonon behavior in Bi-2212 in the $q \to 0$ limit. Moreover, the insights into long-wavelength phonon dynamics revealed in the current work will lead to a deeper understanding of the role of phonons and of electron-phonon coupling in high-T_c superconductivity.

ACKNOWLEDGMENT

The authors would like to acknowledge J. P. Clancy, Department of Physics and Astronomy, McMaster University, Canada, for supplying the samples used in this work.

[1] J. D. Axe and P. Bak, Phys. Rev. B **26**, 4963 (1982).
[2] R. Currat, E. Kats, and I. Luk'yanchuk, Eur. Phys. J. B **26**, 339 (2002).
[3] M. Dzugutov and J. Phillips, J. Non-Cryst. Solids **192–193**, 397 (1995).
[4] W. Finger and T. M. Rice, Phys. Rev. Lett. **49**, 468 (1982).
[5] T. Janssen, O. Radulescu, and A. N. Rubtsov, Eur. Phys. J. B **29**, 85 (2002).
[6] O. Radulescu, T. Janssen, and J. Etrillard, Eur. Phys. J. B **29**, 385 (2002).
[7] P. Miles, S. Kennedy, G. McIntyre, G. Gu, G. Russell, and N. Koshizuka, Phys. C: Supercond. **294**, 275 (1998).
[8] X. B. Kan and S. C. Moss, Acta Cryst. B **48**, 122 (1992).
[9] D. Ariosa, H. Berger, T. Schmauder, D. Pavuna, G. Margaritondo, S. Christensen, R. Kelley, and M. Onellion, Phys. C: Supercond. **351**, 251 (2001).
[10] A. M. Merritt, J.-P. Castellan, T. Keller, S. R. Park, J. A. Fernandez-Baca, G. D. Gu, and D. Reznik, Phys. Rev. B **100**, 144502 (2019).
[11] J. Etrillard, Ph. Bourges, H. F. He, B. Keimer, B. Liang, and C. T. Lin, Europhys. Lett. **55**, 201 (2001).
[12] Y. Wang, J. Wu, J. Zhu, H. Shen, Y. Yan, and Z. Zhao, Physica C **162–164**, 454 (1989).
[13] J. Etrillard, L. Bourges, B. Liang, C. T. Lin, and B. Keimer, Europhys. Lett. **66**, 246 (2004).
[14] B. D. E. McNiven, J. P. F. LeBlanc, and G. T. Andrews, Supercond. Sci. Technol. **34**, 065005 (2021).
[15] J. R. Sandercock, in *Light Scattering in Solids III*, edited by M. Cardona and G. Guntherodt (Springer, Berlin, 1982), Chap. 6, pp. 173–206.
[16] S. Speziale, H. Marquardt, and T. S. Duffy, Rev. Min. Geochem. **78**, 543 (2014).
[17] J. G. Dil, Rep. Prog. Phys. **45**, 285 (1982).
[18] G. T. Andrews, in *Handbook of Porous Silicon*, edited by L. Canham (Springer International, 2018), Chap. 53, pp. 691–703.
[19] B. W. Reed, V. Huynh, C. Tran, and K. J. Koski, Phys. Rev. B **102**, 054109 (2020).

[20] B. W. Reed and K. J. Koski, J. Appl. Phys. **131**, 165109 (2022).
[21] L. E. McNeil and M. Grimsditch, J. Phys.: Condens. Matter **5**, 1681 (1993).
[22] Z. Wang, K. Rolle, T. Schilling, P. Hummel, A. Philipp, B. A. F. Kopera, A. M. Lechner, M. Retsch, J. Breu, and G. Fytas, Angew. Chem. Int. Ed. **59**, 1286 (2020).
[23] M. Boekholt, J. V. Harzer, B. Hillebrands, and G. Güntherodt, Physica C **179**, 101 (1991).
[24] C. E. Bottani and D. Fioretto, Adv. Phys. X **3**, 607 (2018).
[25] F. Chang, P. J. Ford, G. A. Saunders, L. Jiaqiang, D. P. Almond, B. Chapman, M. Cankurtaran, R. B. Poeppel, and K. C. Goretta, Supercond. Sci. Technol. **6**, 484 (1993).
[26] P. Baumgart, S. Blumenröder, A. Erle, B. Hillebrands, P. Splittgerber, G. Güntherodt, and H. Schmidt, Physica C **162–164**, 1073 (1989).
[27] V. V. Aleksandrov1, T. S. Velichkina, V. I. Voronkova, A. A. Gippius, S. V. Rek'ko, I. A. Yakovlev, and V. K. Yanovskii, Solid State Commun. **76**, 685 (1990).
[28] H. Z. Cummins and P. E. Schoen, in *Laser Handbook*, edited by F. T. Arecchi, E. O. Schulz-Dubois, and M. L. Stitch (North-Holland, New York, 1972) Chap. E1, Vol. 2, pp. 1029–1075.
[29] S. Benhabib, Y. Gallais, M. Cazayous, M.-A. Méasson, R. D. Zhong, J. Schneeloch, A. Forget, G. D. Gu, D. Colson, and A. Sacuto, Phys. Rev. B **92**, 134502 (2015).
[30] P. E. Sulewski, P. A. Fleury, and K. B. Lyons, in *Laser Optics of Condensed Matter: The Physics of Optical Phenomena and Their Use as Probes of Matter*, edited by E. Garmire, A. A. Maradudin, and K. K. Rebane (Springer, Boston, 1991), Vol. 2, pp. 121–130.
[31] J. Hwang, T. Timusk, and G. Gu, J. Phys.: Condens. Matter **19**, 125208 (2007).
[32] X. Wang, L. X. You, X. M. Xie, C. T. Lin, and M. H. Jiang, J. Raman Spectrosc. **43**, 949 (2012).
[33] I. Bozovic, Phys. Rev. B **42**, 1969 (1990).
[34] Y. N. Wang, J. Wu, J. S. Zhu, H. M. Shen, J. Z. Zhang, Y. F. Yang, and Z. X. Zhao, in *Beijing International Conference on High Temperature Superconductivity*, edited by Z. X. Zhao, G. J. Cui, and R. S. Han (World Scientific, Beijing, 1989), Vol. 22, pp. 426–429.
[35] S. Sathish, M. Mendik, A. Kulik, G. Gremaud, and P. Wachter, Appl. Phys. Lett. **59**, 167 (1991).
[36] U. Paltzer, D. Schmicker, F. W. de Wette, U. Schroder, and J. P. Toennies, Phys. Rev. B **54**, 11989 (1996).
[37] O. Radulescu and T. Janssen, J. Phys. A **30**, 4199 (1997).
[38] W. Finger and T. M. Rice, Phys. Rev. B **28**, 340 (1983).

Correction: The last sentence of the first paragraph in Sec. III A contained a copyediting error and has been set right.